ISSN 1330-3651 (Print), ISSN 1848-6339 (Online)
https://doi.org/10.17559/TV-20250821002918
Original scientific paper

# A Cascaded Deep Forest Framework for Robust Driver Fatigue Detection using Forehead Electroencephalography

Renyu YANG, Ling ZHANG, Boming ZHONG, Lixing HOU, Donglong ZHU, Jianliang MIN*

**Abstract:** Performance decrement due to fatigue is a leading contributor to traffic accidents and fatalities. Electroencephalogram (EEG) is widely accepted as a reliable physiological indicator of cognitive state, though the application of EEG-based systems in driver monitoring is often limited by the need for multichannel headsets. Forehead EEG, in particular, has emerged as a promising candidate for early detection due to the rise of portable wearable devices. In this work, we propose a robust and efficient method for driver fatigue detection using forehead EEG signals. The approach employs a cascaded deep forest (CDF) framework, incorporating wavelet log-energy entropy and high-order component statistics to extract meaningful features from low-channel EEG signals. A comprehensive labelling protocol was conducted across 26 subjects to validate the method. The experimental results demonstrated a significant improvement in performance, achieving an average accuracy of 95.1%, which outperformed previous studies. Furthermore, the energy characteristics of small-scale oscillations in brain signals across different frequency bands, along with the application of higher-order statistics in the reconstructed phase space, were validated for computational efficiency. This study presented a new framework of using frontal EEG based on a cascade structure to construct a landing fatigue detection method. It could also provide a promising approach for biomedical signal processing in low-channel systems.

**Keywords:** driving fatigue; deep forest; forehead EEG; traffic safety; wearable device

## 1 INTRODUCTION

Fatigue can lead to an inability to continue driving under monotonous conditions and excessive workload, which reduces awareness and attention, thereby increasing the risk of traffic accidents. Common methods for detecting driving fatigue often rely on endogenous and exogenous indicators [1, 2]. External indicators include lane departure detection, facial expression recognition, and posture analysis, though these indicators are influenced by environmental factors such as lighting and driver habits [3]. For example, the Percentage of Eyelid Closure over the Pupil (PERCLOS) is a widely used metric for monitoring driver status [4]. However, the robustness of image-based deep learning methods is limited by individual differences, appearance variation, illumination, and occlusion. In contrast, internal physiological signals, such as EEG, EOG, ECG, and respiration, are less affected by external factors and provide early warnings of fatigue [5]. Among these, EEG is considered a reliable indicator of driving fatigue, as it reflects cognitive changes and has been extensively studied for fatigue detection [6, 7].

EEG is a record of the spontaneous and rhythmic electrical discharges of neurons on the surface of the scalp in the brain. It has the advantages of high temporal resolution, strong reliability, and low cost, and is frequently used in driving fatigue research for reliable monitoring. Previous studies explore EEG spectral features and their relation to mental states. For instance, Subasi et al. [8] described a fatigue detection model based on EEG band changes. Wan et al. [9] examined the impact of varying anger intensities on EEG power spectrum and sample entropy patterns in naturalistic driving scenarios. In addition, multiple deep learning algorithms for processing multichannel EEG signals have been developed [10, 11]. Conventional multi-channel EEG systems (e.g., 32/64-channel configurations) are confined to controlled laboratory settings due to their dependency on scalp electrodes within hair-bearing regions. This design precludes real-world deployment in driving environments and impedes widespread adoption. The emergence of wearable neurotechnology has thus prioritized electrode minimization and hair-free placements.

With the rise of mobile medical electronics, wearable solutions are evolving to minimize electrode count and prioritize hair-free sites. Forehead EEG provides an optimal trade-off between operational practicality and signal fidelity. Scientifically, the prefrontal cortex - directly underlying the forehead - is a well-established neural substrate for sustained attention [12]. Critically, driver fatigue robustly exhibits increased $\theta$-band (4-8 Hz) oscillations within this region, a signature accessible via forehead electrodes without full-scalp coverage. Practically, hair-free placement ensures both signal stability and user comfort, while enabling seamless integration into consumer-grade dry-electrode systems [13]. Consequently, forehead channels capture discriminative fatigue markers while overcoming the limitations of traditional EEG configurations. Nevertheless, low-channel recordings remain challenging because spatial information is drastically reduced [14]. For example, Fan et al. [15] extract energy, entropy, rhythmic energy ratio, and frontal asymmetry ratio from forehead EEG for fatigue detection, while Liu et al. [16] utilize power spectral density (PSD), functional connectivity, and entropy across three frontal channels. Multi-source features, such as facial vision, have also been fused with forehead EEG [17]. However, the accuracy and real-time performance of the above researches for practical application in detecting driving fatigue still need to be improved. This can be attributed mainly to two factors: first, the reduced number of electrodes restricts the spatial information available, making it challenging to capture sufficient dynamic patterns associated with fatigue-related brain activities. Second, many existing models rely on complicated features and classifiers that lack robustness against subject variability and do not account for the real-time requirement. Therefore, advancing fatigue detection methods based on forehead EEG - by improving both feature representation and computational efficiency - would hold significant promise for practical driving fatigue monitoring.

The current work aims to build an applicable, efficient, and robust driver fatigue detection method for a low-channel forehead EEG-based system. Two fast and effective features based on the energy information of the small-scale oscillations of brain signals from different frequency bands and the higher-order statistics of the nonlinear dynamic state from the reconstructed phase space are proposed. Ensemble learning in a cascaded deep forest is utilized to further improve the robustness of the prediction. In addition, a comprehensive labelling engineering approach is employed to enhance data ground truth across 26 subjects. The results show that the proposed framework achieves good recognition performance, which can be adapted to low-channel EEG-based driving fatigue detection.

## 2 METHODS

### 2.1 Participants and Experimental Procedure

Twenty-six healthy subjects (aged 18 to 24 years; 12 males and 14 females) participated in a simulated driving experiment. Each held a driving license of C1. Subjects were instructed to abstain from stimulants such as alcohol, coffee, or tea, and to keep a normal sleep schedule. The subjects who participated in this work are approved by the institutional research ethics committee in accordance with the Declaration of Helsinki. The experiment is conducted using a static driving simulator as depicted in Fig. 1a. During the experiment, an EEG cap is fitted to each subject's scalp to record brain activity, and a hemispheric webcam is employed to monitor facial expressions. In addition, the subjects are inquired every 20 minutes for fatigue scales. The driving simulation software also provides individual practice scores based on the participants' driving performance. The driving scenario involves a highway with low traffic volume, which contributes to a monotonous and drowsy driving experience, with the entire task lasting nearly two hours.

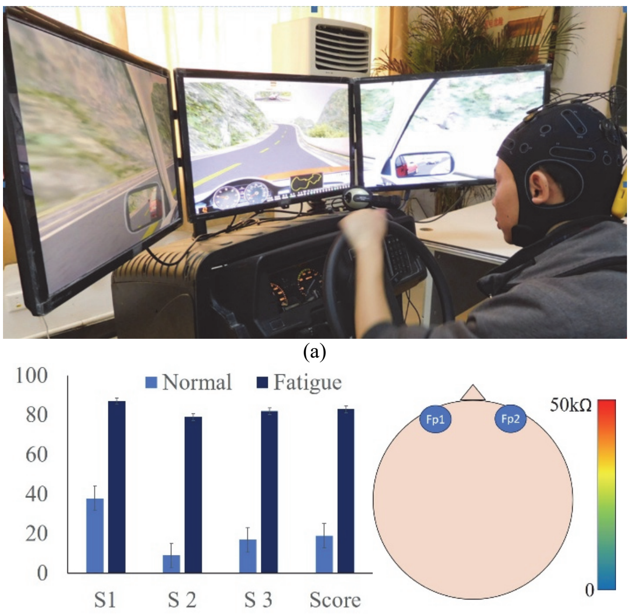


**Figure 1** Experimental setting: (a) driving surround; (b) evaluation score; (c) forehead channels

### 2.2 Data Acquisition and Preprocessing

The related data is publicly available online at https://figshare.com/articles/dataset/The_raw_EEG_recordings_used_for_detecting_driver_fatigue_/27926826. It is recorded with a Neuroscan system of 40 electrodes at a sampling frequency of 1000 Hz. Although full scalp coverage is implemented, prefrontal channels ($Fp_1$/$Fp_2$) are prioritized for signal acquisition due to their sensitivity to fatigue-related neural activity and their practical feasibility in wearable applications. The electrode placement adheres to the standard international 10/20 system, referenced to the right earlobe. Skin impedance of each electrode is meticulously adjusted to below 5 kΩ using conductive gel (dark blue) as shown in Fig. 1c. Based on fatigue scores, two states are defined in the comprehensive evaluation: data from the 5-minute interval preceding a low-score timestamp is labelled as the normal state, whereas data from the 5-minute interval preceding a high-score timestamp is labelled as the fatigue state. In Fig. 2, as described in [6], signal preprocessing is carried out. In particular, eyeblink artifacts are removed using a wavelet-based unsupervised method [18]. Finally, EEG signals are segmented into 1-second epochs without overlap. The segmentation results in a total of 15,600 epochs across 26 subjects for each forehead channel.

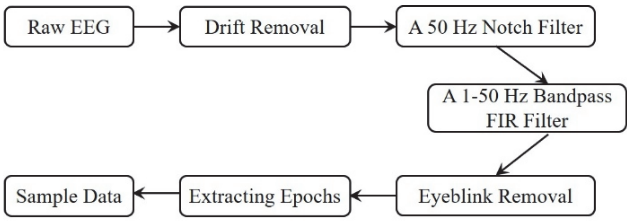


**Figure 2** The data preprocessing steps

### 2.3 Comprehensive Evaluation of Fatigue

The comprehensive fatigue score was derived by averaging three fatigue-related scores: $S1$, $S2$, and $S3$. $S1$: it is a centesimal drowsiness-related score, quantifying facial expressions captured by video analysis. Key indicators included the PERCLOS, blinking frequency, head posture and yawning. According to the literature [19], these components were respectively assigned weights of 30%, 30%, 20% and 20%. Fuzzy logic is used to categorize each variable into small, medium or large levels. Then the final $S1$ score was obtained based on the weighted average. $S2$: it originates from the simulation driving software, starting at 100 points and decreasing based on deductions for driving errors such as road deviations and overspeed. And it was reversed so that a higher value corresponds to a higher level of fatigue. $S3$: a common questionnaire score, widely used in EEG-based fatigue studies [6, 20]. The average score of these parameters was depicted in Fig. 1b. A higher cumulative fatigue score indicates a more pronounced level of driving fatigue. Based on the score, EEG data collected prior to the score-related time was finally categorized as representing either a normal state or a fatigue state.

### 2.4 Feature Construction

Entropy has been widely used in EEG signal analysis [6, 21]. The wavelet log-energy entropy (WLE) is a combination of wavelet transform and entropy. The former improves the time-frequency resolution by adaptively selecting the corresponding frequency band to match the frequency spectrum of the signal. The combination can provide the energy information of different frequency bands in EEG. The process of WLE was shown in Fig. 3a. In detail, the cA1 and cD1 represented approximate coefficients and detail coefficients obtained by the 1-th layer of wavelet decomposition. It respectively described the low and high frequency components of the signal. Similarly, a series of approximate and detail coefficients can be obtained by iterating this process. Then, the log-energy entropy was calculated according to the corresponding coefficients. Finally, feature fusion was carried out in the feature layer. The formula of $WLE_i$ is as follows:

$$WLE_i = \sum_j \log(c_{i,j}{}^2) \tag{1}$$

where $c_{i,j}$ is the wavelet decomposition coefficient of the $i$-th leaf node in the wavelet tree. Here, the value of $i$ is the number of decomposed layers plus 1.

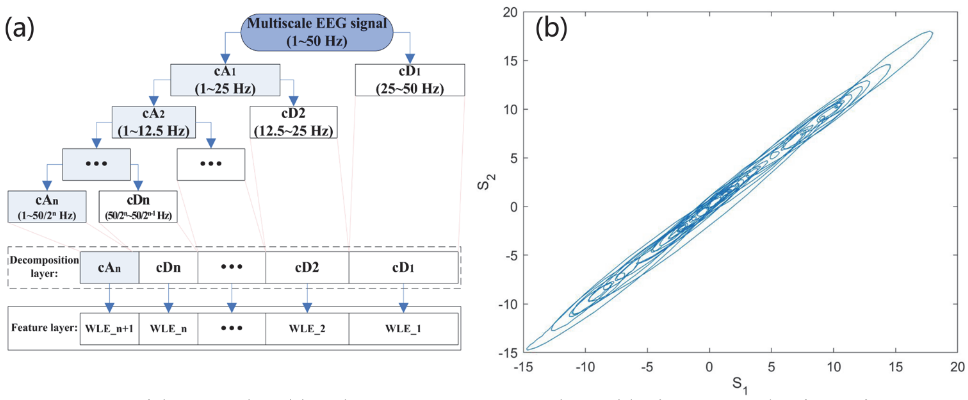


**Figure 3** EEG feature profiles: (a) the feature extraction process of WLE; (b) a 2-D diagram of RPS in EEG epoch

In order to acquire an amount of information about the dynamic state from signal epoch, the reconstructed phase space (RPS) was applied to obtain some dynamic features. It is a very useful tool for the extraction of the nonlinear dynamic state of the signal [22], with an intuitive representation of the evolution of the dynamic behavior of the signal over time (shown in Fig. 3b). For a given $N$-point time series $\{s_i, 1 \le i \le N\}$, it can embed $S_i$ into a reconstruction matrix using the delay coordinated $\tau$ as follows:

$$S = \left\{ S_i | S_i = \left[ s_i, s_{i+\tau}, \cdots, s_{i+(m-1)\tau} \right]^T, i = 1, 2, \cdots, N-(m-1)\tau \right\} = \begin{bmatrix} s_1 & s_2 & \cdots & s_{N-(m-1)\tau} \\ s_{1+\tau} & s_{2+\tau} & \cdots & s_{N-(m-1)\tau+\tau} \\ \cdots & \cdots & \cdots & \cdots \\ s_{1+(m-1)\tau} & s_{2+(m-1)\tau} & \cdots & s_N \end{bmatrix} \tag{2}$$

where the $\tau$ is set to 1 in most literature studies and the dimension m is an integer value greater than or equal to 2. Furthermore, the principal component analysis (PCA) was then used to obtain main components and calculate four statistical features, namely the standard deviation ($SD$), the interquartile range ($IQR$), the sample skewness ($SS$) and the sample kurtosis ($SK$). The formula defined as follows:

$$SD = \sqrt{\frac{1}{N-1}\sum_{i=1}^{N} \left| P_i - \mu \right|^2} \tag{3}$$

$$SS = \frac{\frac{1}{N}\sum_{i=1}^{N}\left(P_i - \mu\right)^3}{SD^3} \tag{4}$$

$$SK = \frac{\frac{1}{N}\sum_{i=1}^{N}\left(P_i - \mu\right)^4}{SD^4} \tag{5}$$

where $P_i$ is the information value of each component based on the principal component analysis, $\mu$ is the mean of $P_i$, and $N$ is the number of components. IQR is the difference between the 25th and 75th percentiles of the data contained in the component. Due to the phase space representation diagram, we can obtain component statistical features (CSF) about the concise dynamic distribution information from the whole signal system.

For feature parameterization, this study employs fourteen well-established wavelet bases - db4, db5, coif3, coif5, sym5, sym8, bior2.4, bior3.3, bior4.4, bior5.5, rbio2.4, rbio3.3, rbio3.5 and rbio5.5 - for wavelet log-energy entropy (WLE) and consistently performs a four-level decomposition. These bases have been widely used in EEG analyses [23, 24] and provide sufficient time-frequency resolution to capture fatigue-related rhythms. The four-level decomposition covers $\delta$, $\theta$, $\alpha$, $\beta$ and $\gamma$ bands that are highly relevant to fatigue detection. In reconstructed phase space (RPS), the delay $\tau$ is set to 1 and the embedding dimension m is constrained to 2-15, as $\tau$ = 1 has been shown to adequately reveal the dynamical evolution of EEG signals, while this $m$-range balances nonlinear characterization against computational cost. To improve generalization and reduce overfitting, a parameter bank was constructed and a stochastic feature generator (SFG) randomly draws parameter configurations in each cascade layer. Although the selection is random, the cascaded forest evaluates the utility of each configuration and retains those that enhance classification, thereby achieving self-optimizing screening without additional computational burden and improving robustness.

## 2.5 Classification Algorithm

A cascaded deep forest model was employed to yield the excellent performance with a manageable cost [25]. It uses a multi-layer structure, where each layer consists of multiple random forests. They learn the feature information from the input feature vectors and pass the processed information to the next layer. Each layer selects various types of random forests to enhance the model's generalization capability by parameter perturbation. The proposed model was composed of a feature vector of SFG, a cascade forest structure and a final output as shown in Fig. 4. The SFG module was used to generate a feature vector at the current level according to the input signal. Then the class probability joint vector in the previous level and the new input feature vector generated by SFG were used as the next level input.

Until the last level, the final class probability values can be used to determine the final prediction for multiple learners. In this process, each level of the cascade consisted of two RF and two ET learners to boost the randomness and diversity of model. RF delivers the robust prediction through the bootstrap aggregation and feature subset optimization, while ET enhances the model's ability to explore the underlying data structure via fully random node splitting. This combination can achieve an effective balance between bias and variance, enriching feature representation and improving the model's generalization performance. In addition, the number of cascade levels can be adaptively determined by the trend of evaluation metric.

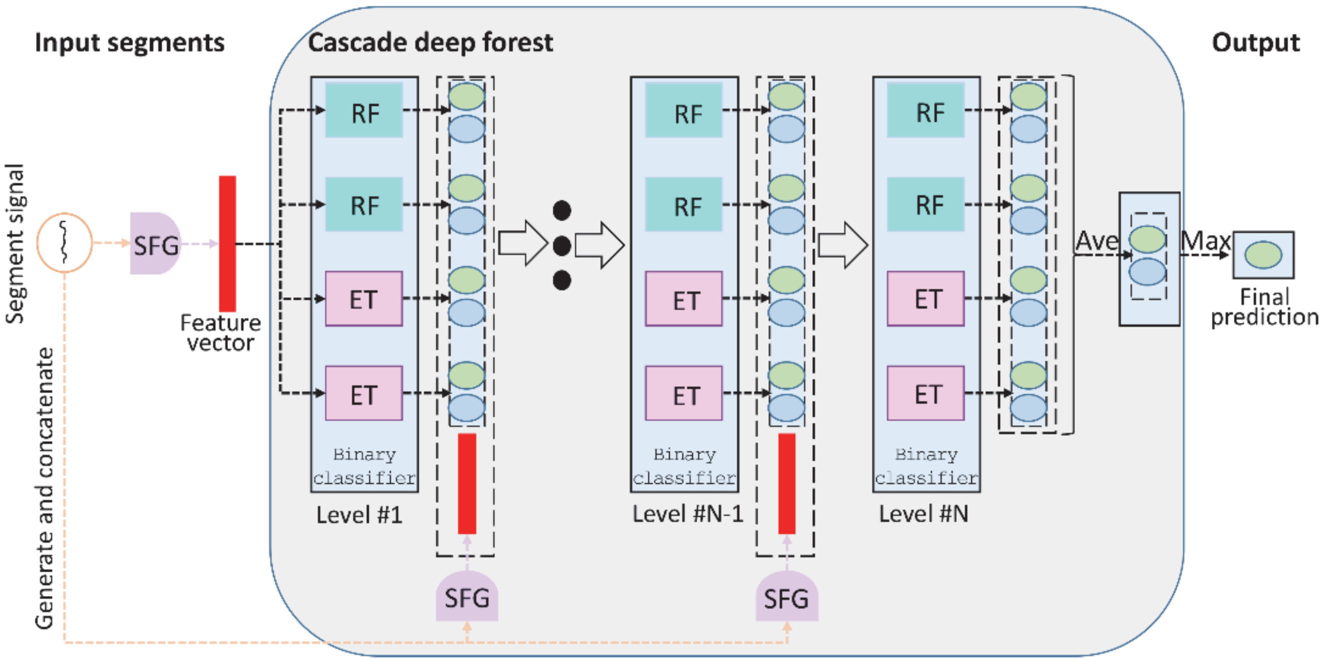


**Figure 4** The cascaded deep forest structure. In the core of this model, each layer had two RF and two ET classifiers, and different layers own the same structure

## 2.6 Evaluation and Settings

It involves the accuracy ($Acc$), the sensitivity ($Sn$), the specificity ($Sp$), and the Matthews correlation coefficient ($MCC$) in the leave-one-out cross validation (LOO). In addition, the statistical hypothesis test and two one-factor repeated-measures ANOVAs are applied to assess statistical significance. The receiver operating characteristic (ROC) curve and the precision-recall (PR) curve are created to visually display the classification quality. Their area under the corresponding curve indicates that the closer the value is to 1, the better the observed result.

$$Acc = \frac{TP + TN}{TP + FP + FN + TN} \tag{6}$$

$$Sn = \frac{TP}{TP + FN} \tag{7}$$

$$Sp = \frac{TP}{TP + FP} \tag{8}$$

$$MCC = \frac{TP \times TN - FP \times FN}{\sqrt{(TP + FP)(TP + FN)(TN + FP)(TN + FN)}} \tag{9}$$

where $TP$ is true positive, $TN$ is true negative, $FN$ is false negative and $FP$ is false positive.

They were conducted in the Python 3.7 environment and performed on a 64-bit Windows 8.1 OS desktop with an Intel (R) Core (TM) i7-7700K @4.20 GHz CPU and 4 GB RAM.

# 3 EXPERIMENTAL RESULTS

## 3.1 The Overall Performance

The fusion feature of WLE and CSF was input into a CDF with a robust parameter tuning. In addition, LR is frequently employed as a benchmark algorithm. SVM is also commonly used for the high-precision classification of small samples. RF and ET are two simple but well-generalized tree model classification methods. Specially, lightGBM is a very promising tree boosting algorithm due to its high efficiency and ease-of-parallel capacity. Therefore, the performance of our model was compared with these classical classifiers to assess the effectiveness in

Tab. 1. It showed the comparative results by LOO. The proposed model demonstrated the superior performance with an average *Acc* of 95.1% (±4.43), *Sn* of 94.9% (±4.96), *Sp* of 95.3% (±4.32), and *MCC* of 90.2% (±8.82). While the average results of other models were 93.8% of *Acc*, 93.3% of *Sn*, 94.3% of *Sp* and 87.6% of *MCC*. Furthermore, a paired-sample *t*-test with a significance level of $\alpha = 0.05$ was conducted between these classifiers. The results demonstrated the significant difference of our model over other classifiers ($p < 0.01$). In particular, the comparison between CDF and lightGBM showed a statistically significant difference ($t_{stat} = 2.45$, $p = 0.0061$).

**Table 1** Performance compared with other models

| Metrics | LR | SVM | RF | ET | lightGBM | CDF |
|---|---|---|---|---|---|---|
| Acc | 92.9 ± 7.58 | 92.8 ± 7.69 | 94.2 ± 5.27 | 94.2 ± 5.40 | 94.8 ± 4.94 | 95.1 ± 4.43 |
| Sn | 92.5 ± 7.93 | 92.3 ± 8.24 | 93.6 ± 6.17 | 93.4 ± 6.39 | 94.5 ± 5.31 | 94.9 ± 4.96 |
| Sp | 93.4 ± 7.28 | 93.3 ± 7.24 | 94.8 ± 4.96 | 95.0 ± 5.00 | 95.1 ± 4.92 | 95.3 ± 4.32 |
| MCC | 85.9 ± 15.2 | 85.6 ± 15.4 | 88.4 ± 10.5 | 88.4 ± 10.7 | 89.7 ± 9.84 | 90.2 ± 8.82 |

**Table 2** Influence of different basis functions on the calculation time of each epoch for WLE

| Basis function | db4 | db5 | coif3 | coif5 | sym5 | sym8 | bior2.4 |
|---|---|---|---|---|---|---|---|
| Time / s | 0.0033 | 0.0033 | 0.0034 | 0.0034 | 0.0033 | 0.0034 | 0.0037 |
| Basis function | bior3.3 | bior4.4 | bior5.5 | rbio2.4 | rbio3.3 | rbio3.5 | rbio5.5 |
| Time / s | 0.0038 | 0.0039 | 0.0039 | 0.0038 | 0.0039 | 0.0039 | 0.0039 |

Furthermore, the individual performance was illustrated in Fig. 5. It revealed that the CDF exhibited a robustness across the entire subjects. When compared with other classifiers, the result of CDF showed an improvement to some extent due to the cascaded deep tree structure. In order to provide a more detailed insight, a graphical show including the ROC and PR was presented in Fig. 6. The high scores in AUC and AP highlighted the ability of models to accurately distinguish between true positives and negatives as well as false positives and negatives.

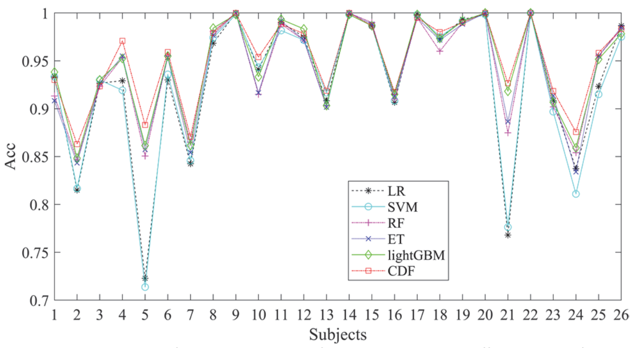


**Figure 5** The classification accuracy of each subject with different classifiers

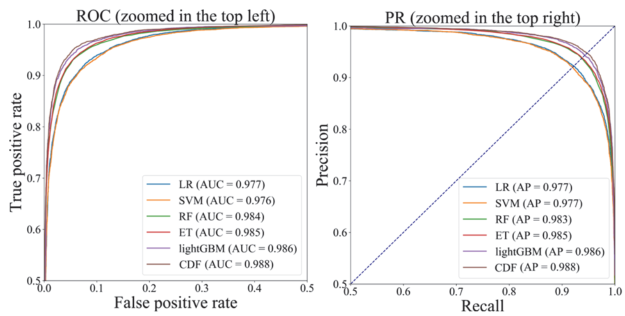


**Figure 6** The results of different models in terms of ROC and PR

## 3.2 Feature Impact on Model Efficacy

The efficiency of feature processing in terms of computational time is a critical yet often overlooked aspect in related research. The impact of feature parameters on computational time is detailed in Tab. 2 and 3. Notably, most feature calculations were completed within less than 0.005 seconds. Specifically, the computation time for WLE remained stable, while CSF exhibited a slight and linear increase. This indicates that the feature extraction process using WLE and CSF is both rapid and holds potential for real-time fatigue detection in low-channel EEG systems.

In addition, the classification performance using single WLE or CSF was evaluated in Fig. 7. It can be observed that all average accuracies exceeded 90% and 92% respectively for WLE and CSF. To further compare the difference, separate one-factor repeated-measure ANOVAs was performed. For multiple comparison testing, the Bonferroni method was utilized. As illustrated in Fig. 9a, the results revealed significant differences ($F_{stat} = 4.45$, $p = 0.0124$). In detail, the multiple comparison test revealed a notable difference between the combined WLE+CSF feature and WLE alone, whereas no significant deviation was observed in comparison with CSF.

Moreover, the boxplot showed that the results based on the fused features had a robust performance. In conclusion, that the feature extraction methods combining sub-band energy information of multi-waves and multi-order statistical features of RPS demonstrated both efficiency and usefulness for EEG data analysis. Furthermore, these approaches hold potential as a reference framework for analysing other types of physiological signals.

## 3.3 Single-Channel Performance Analysis

Recently, the use of single-channel EEG devices has gained an increasing attention for the simplicity and user-friendliness. A comparison of performance using the channel $Fp_1/Fp_2$ was presented in Fig. 8. The performance of $Fp_2$ was better than that of using $Fp_1$, which obtained the best result with an *Acc* of 91.4%, *Sn* of 90.6%, *Sp* of 92.1% and *MCC* of 82.9%. There were significant differences between $Fp_1 + Fp_2$ and $Fp_1$, and between $Fp_1 + Fp_2$ and $Fp_2$ in Fig. 9b ($F_{stat} = 10.44$, $p = 4.12e^{-05}$). It suggested that that using forehead EEG from two channels based on CDF can significantly improve performance in the identification of fatigue compared to that of single channel. The signals from more spatial resolutions are helpful for the model to obtain stable features to improve the recognition ability.

**Table 3** Influence of the added embedding dimension on the calculation time of each epoch for CSF

| Dimension | 2 | 3 | 4 | 5 | 6 | 7 | 8 |
|---|---|---|---|---|---|---|---|
| Time / s | 0.0021 | 0.0023 | 0.0027 | 0.0031 | 0.0035 | 0.0040 | 0.0043 |
| Dimension | 9 | 10 | 11 | 12 | 13 | 14 | 15 |
| Time / s | 0.0048 | 0.0051 | 0.0056 | 0.0059 | 0.0063 | 0.0068 | 0.0073 |

**Table 4** Performance comparison with previous studies

| Author | Feature | Cross validation | Sample size | Channel | Acc / % |
|---|---|---|---|---|---|
| Luo [20] | Multiscale FE | Hold-out | 16 | $Fp_1$ and $Fp_2$ | 95.4 |
| Mu [30] | FE | 10-fold | 15 | $Fp_1$ and $Fp_2$ | 85.0 |
| Ogino [31] | PSD and ME | 10-fold | 29 | $Fp_1$ | 72.7 |
| Jalilifard [32] | STFT and SE | Hold-out | 10 | $Fpz$ and $Cz$ | 91.0 |
| This paper | WLE and CSF | LOO | 26 | $Fp_1$ and $Fp_2$ | 95.1 |

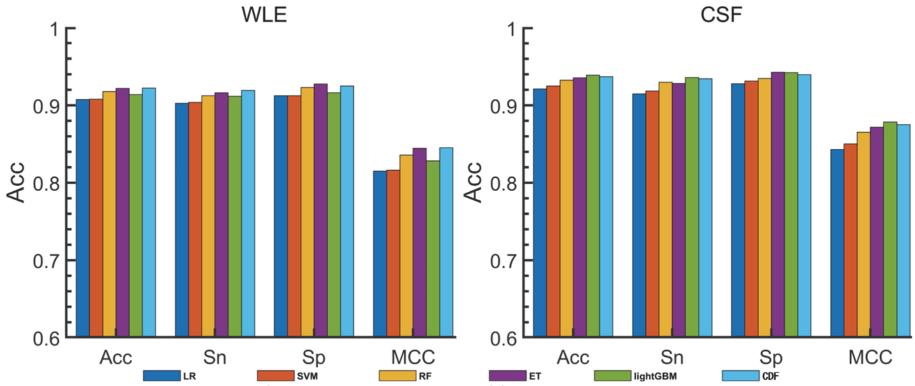


**Figure 7** Comparison using WLE and CSF with the combined channel

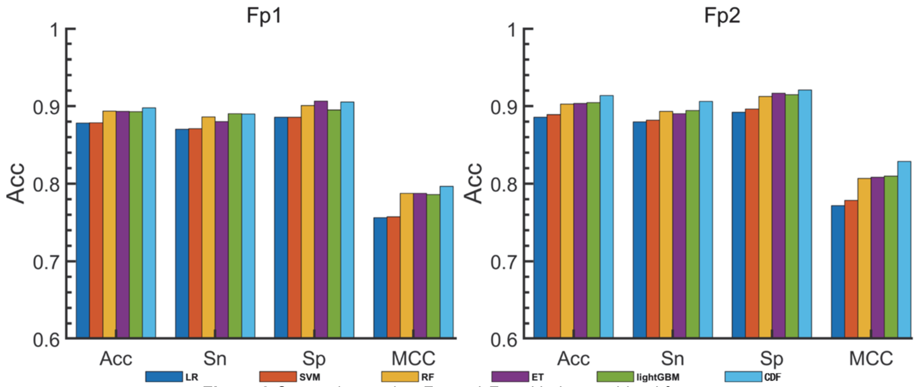


**Figure 8** Comparison using $Fp_1$ and $Fp_2$ with the combined feature

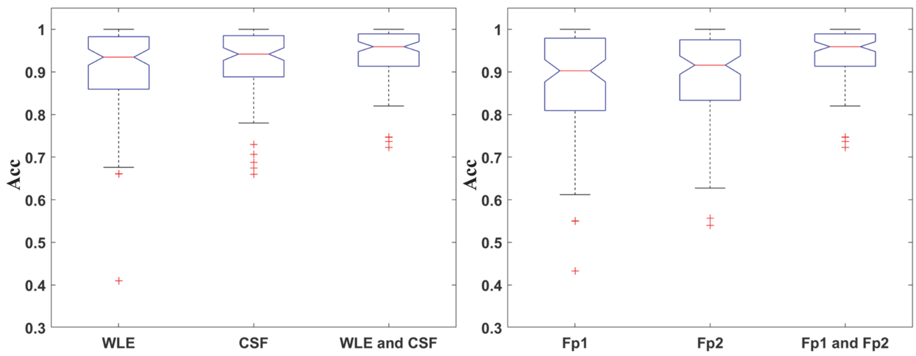


**Figure 9** Boxplot of three groups in feature and channel groups

## 4 DISCUSSION

While multi-channel EEG systems continue to develop in driving fatigue research, wearable applications increasingly adopt low- or single-channel solutions. Forehead EEG balances convenience and comfort, aligning with consumer-grade BCI devices that typically include forehead electrodes [26]. However, feature extraction remains a major challenge in such limited-channel systems. Beyond computational efficiency, the selected features also have clear physiological relevance to neural activity under fatigue. Wavelet log-energy entropy (WLE) quantifies the energy distribution across EEG frequency bands, and fatigue is typically characterized by increased $\theta$ activity and decreased $\alpha$ and $\beta$ activity in the frontal region [27]; these spectral alterations are effectively captured by WLE. Meanwhile, component statistical features (CSF) derived from the reconstructed phase space represent the nonlinear dynamics of EEG signals. Fatigue often reduces neural complexity, which is reflected in changes in skewness, kurtosis, and other higher-order statistics. Thus, the combination of WLE and CSF not only enhances the discrimination between alert and fatigue states but also provides neurophysiological interpretability of the proposed method. Experimental results further confirmed that these features meet the requirements for real-time fatigue detection as shown in Tabs. 2 and 3 and Fig. 7: both WLE and CSF achieved high computational efficiency and accuracy. It demonstrated their practical suitability for low-channel EEG systems.

Experimental results indicated that the $Fp_2$ electrode was most suitable for a single-channel EEG-based driver fatigue detection system in Fig. 8. The prefrontal region with both $Fp_1$ and $Fp_2$ can further improve the stability of prediction. The forehead shows a dominant activity during alert states, whereas posterior region (e.g., O1/O2) becomes much active during fatigue [28, 29]. However, forehead electrodes are preferred due to the hair-free placement, stable signal acquisition and wearing comfort. Future studies can incorporate the occipital region via a circle headband device to further enhance the robustness.

In addition, recent studies have utilized prefrontal EEG for driver fatigue detection (Tab. 4). Mu et al. [30] achieved an accuracy of 85.0% using fuzzy entropy (FE). Our previous research, however, achieved an accuracy of 93.9% using multi-entropies. In addition, Luo et al. [20] reported a performance of 95.4% using an adaptive multiscale fuzzy entropy method. Despite the high performance of FE in fatigue detection, its computational cost limits its suitability for real-time monitoring. While other studies have explored various entropy-based methods such as multiscale entropy (ME) and Shanon entropy (SE) [31, 32], the proposed method demonstrates superior performance in forehead-EEG-based driving fatigue detection.

Although this study provides valuable insights into forehead-EEG-based signal analysis in fatigue detection, three limitations remain: (1) Owing to experimental constraints, the sample size is still limited; we will therefore expand data collection to include participants of different ages, genders, and driving experiences to improve the generalizability of the approach. (2) In real-world driving environments, forehead EEG is susceptible to ocular, perspiration, and motion artifacts; future work will adopt a hybrid artifact-suppression pipeline that combines independent component analysis with deep auto-encoders and will evaluate improved dry-electrode designs for enhanced signal quality. (3) Single-modal EEG may be insufficient to fully characterize driving fatigue; we will therefore explore multimodal fusion strategies that integrate vehicle operational parameters, eye-movement features, and machine-vision cues, and validate the framework in on-road driving scenarios to further improve model robustness and practicality.

## 5 CONCLUSION

With the advancement of vehicle intelligence, monotonous driving environments can easily induce fatigue. This study proposed an efficient feature extraction method based on low-channel prefrontal EEG signals, combining wavelet transform-derived frequency band energy entropy and high-order statistical features from the phase space reconstruction to automatically detect driver fatigue. A cascaded deep forest framework was designed to enhance prediction accuracy and model robustness. Compared to conventional methods, this approach was faster and more accurate, with experimental results demonstrating its computational efficiency and reliable predictive capability. This portable EEG-based detection technology offers a novel solution for driver fatigue monitoring and can be extended to other wearable brain-computer interface applications.

### Acknowledgements

This work was supported by Humanity and Social Science Planning Fund of Ministry of Education (24YJAZH194); the Scientific Research Projects of Guangdong Provincial Department of Education - Special Projects in key areas (2024ZDZX3055); the National Statistical Science Research Project (2025LZ033); and the Natural Science Foundation of Guangdong Province (2023A1515011021).

## 6 REFERENCES

[1] Doudou, M., Bouabdallah, A., & Berge-Cherfaoui, V. (2020). Driver drowsiness measurement technologies: Current research, market solutions, and challenges. *International Journal of Intelligent Transportation Systems Research*, *18*, 297-319. https://doi.org/10.1007/s13177-019-00199-w

[2] Zhang, Z., Ning, H., & Zhou, F. (2022). A systematic survey of driving fatigue monitoring. *IEEE Transactions on Intelligent Transportation Systems*, *23*(11), 19999-20020. https://doi.org/10.1109/TITS.2022.3189346

[3] Němcová, A., et al. (2020). Multimodal features for detection of driver stress and fatigue: review. *IEEE Transactions on Intelligent Transportation Systems*, *22*(6), 3214-3233. https://doi.org/10.1109/TITS.2020.2977762

[4] Dasgupta, A., Rahman, D., & Routray, A. (2018). A smartphone-based drowsiness detection and warning system for automotive drivers. *IEEE Transactions on Intelligent Transportation Systems*, *20*(11), 4045-4054. https://doi.org/10.1109/TITS.2018.2879609

[5] Lal, S. K. L., & Craig, A. (2002). Driver fatigue: electroencephalography and psychological assessment. *Psychophysiology*, *39*(3), 313-321. https://doi.org/10.1017/S0048577201393095

[6] Min, J., Xiong, C., Zhang, Y. et al. (2021). Driver fatigue detection based on prefrontal EEG using multi-entropy measures and hybrid model. *Biomedical Signal Processing and Control*, *69*, 102857. https://doi.org/10.1016/j.bspc.2021.102857

[7] Lan, Z., Zhao, J., Liu, P., et al. (2024). Driving fatigue detection based on fusion of EEG and vehicle motion information. *Biomedical Signal Processing and Control*, *92*, 106031. https://doi.org/10.1016/j.bspc.2024.106031

[8] Subasi, A., Saikia, A., Bagedo, K. et al. (2022). EEG-based driver fatigue detection using FAWT and multiboosting approaches. *IEEE Transactions on Industrial Informatics*, *18*(10), 6602-6609. https://doi.org/10.1109/TII.2022.3167470

[9] Wan, P., Jing, X., Lu, S., & Yan, L. (2023). Impact of temperament types and anger intensity on drivers' EEG power spectrum and sample entropy: an on-road evaluation toward road rage warning. *Tehnički vjesnik*, *30*(4), 1055-1067. https://doi.org/10.17559/TV-20221021054632

[10] Gao, Z., Wang, X., Yang, Y. et al. (2019). EEG-based spatio–temporal convolutional neural network for driver

fatigue evaluation. *IEEE Transactions on Neural Networks and Learning Systems*, *30*(9), 2755-2763. https://doi.org/10.1109/TNNLS.2018.2886414

[11] Othmani, A., Sabri, A. Q. M., Aslan, S. et al. (2023). EEG-based neural networks approaches for fatigue and drowsiness detection: A survey. *Neurocomputing*, 126709. https://doi.org/10.1016/j.neucom.2023.126709

[12] Lin, C. T., Chuang, C. H., Cao, Z., et al. (2017). Forehead EEG in support of future feasible personal healthcare solutions: Sleep management, headache prevention, and depression treatment. *IEEE Access*, *5*, 10612-10621. https://doi.org/10.1109/ACCESS.2017.2675884

[13] Dimitrakopoulos, G. N., Kakkos, I., Dai, Z., et al. (2018). Functional connectivity analysis of mental fatigue reveals different network topological alterations between driving and vigilance tasks. *IEEE Transactions on Neural Systems and Rehabilitation Engineering*, *26*(4), 740-749. https://doi.org/10.1109/TNSRE.2018.2791936

[14] Balam, V. P. (2024). Systematic review of single-channel EEG-based drowsiness detection methods. *IEEE Transactions on Intelligent Transportation Systems*, *25*(11), 15210-15227. https://doi.org/10.1109/TITS.2024.3442249

[15] Fan, C., Peng, Y., Peng, S., Zhang, H., Wu, Y., & Kwong, S. (2021). Detection of train driver fatigue and distraction based on forehead EEG: a time-series ensemble learning method. *IEEE Transactions on Intelligent Transportation Systems*, *23*(8), 13559-13567. https://doi.org/10.1109/TITS.2021.3125737

[16] Liu, X., Li, G., Wang, S. et al. (2021). Toward practical driving fatigue detection using three frontal EEG channels: A proof-of-concept study. *Physiological Measurement*, *42*(4), 044003. https://doi.org/10.1088/1361-6579/abf336

[17] Min, J., Cai, M., Gou, C. et al. (2023). Fusion of forehead EEG with machine vision for real-time fatigue detection in an automatic processing pipeline. *Neural Computing and Applications*, *35*(12), 8859-8872. https://doi.org/10.1007/s00521-022-07466-0

[18] Khatun, S., Mahajan, R., & Morshed, B. I. (2016). Comparative study of wavelet-based unsupervised ocular artifact removal techniques for single-channel EEG data. *IEEE Journal of Translational Engineering in Health and Medicine*, *4*, 1-8. https://doi.org/10.1109/JTEHM.2016.2544298

[19] Dong, Y., Hu, Z., Uchimura, K. et al. (2010). Driver inattention monitoring system for intelligent vehicles: A review. *IEEE Transactions on Intelligent Transportation Systems*, *12*(2), 596-614. https://doi.org/10.1109/TITS.2010.2092770

[20] Luo, H., Qiu, T., Liu, C. et al. (2019). Research on fatigue driving detection using forehead EEG based on adaptive multi-scale entropy. *Biomedical Signal Processing and Control*, *51*, 50-58. https://doi.org/10.1016/j.bspc.2019.02.005

[21] Chaudhuri, A. & Routray, A. (2019). Driver fatigue detection through chaotic entropy analysis of cortical sources obtained from scalp EEG signals. *IEEE Transactions on Intelligent Transportation Systems*, *21*(1), 185-198. https://doi.org/10.1109/TITS.2018.2890332

[22] Darjani, N. & Omranpour, H. (2020). Phase space elliptic density feature for epileptic EEG signals classification using metaheuristic optimization method. *Knowledge-Based Systems*, *205*, 106276. https://doi.org/10.1016/j.knosys.2020.106276

[23] Menshawy, M. E. L., Benharref, A., & Serhani, M. (2015). An automatic mobile-health based approach for EEG epileptic seizures detection. *Expert Systems with Applications*, *42*(20), 7157-7174. https://doi.org/10.1016/j.eswa.2015.04.068

[24] Chinara, S. (2021). Automatic classification methods for detecting drowsiness using wavelet packet transform extracted time-domain features from single-channel EEG signal. *Journal of Neuroscience Methods*, *347*, 108927. https://doi.org/10.1016/j.jneumeth.2020.108927

[25] Zhou, Z. H. & Feng, J. (2019). Deep forest. *National Science Review*, *6*(1), 74-86. https://doi.org/10.1093/nsr/nwy108

[26] Maskeliunas, R., Damasevicius, R., Martisius, I., et al. (2016). Consumer-grade EEG devices: are they usable for control tasks? *PeerJ*, *4*, e1745. https://doi.org/10.7717/peerj.1746

[27] Borghini, G., Astolfi, L., Vecchiato, G., Mattia, D., & Babiloni, F. (2014). Measuring neurophysiological signals in aircraft pilots and car drivers for the assessment of mental workload, fatigue and drowsiness. *Neuroscience & Biobehavioral Reviews*, *44*, 58-75. https://doi.org/10.1016/j.neubiorev.2012.10.003

[28] Wang, F., Ma, M., & Zhang, X. (2024). Study on a portable electrode used to detect the fatigue of tower crane drivers in real construction environment. *IEEE Transactions on Instrumentation and Measurement*, *73*, 1-14. https://doi.org/10.1109/TIM.2024.3353274

[29] Wei, C. S., Wang, Y. T., Lin, C. T. et al. (2018). Toward drowsiness detection using non-hair-bearing EEG-based brain-computer interfaces. *IEEE Transactions on Neural Systems and Rehabilitation Engineering*, *26*(2), 400-406. https://doi.org/10.1109/TNSRE.2018.2790359

[30] Mu, Z., Hu, J., & Yin, J. (2017). Driving fatigue detecting based on EEG signals of forehead area. *International Journal of Pattern Recognition and Artificial Intelligence*, *31*(5), 1750011. https://doi.org/10.1142/S0218001417500112

[31] Ogino, M. & Mitsukura, Y. (2018). Portable drowsiness detection through use of a prefrontal single-channel electroencephalogram. *Sensors*, *18*(12), 4477. https://doi.org/10.3390/s18124477

[32] Jalilifard, A. & Pizzolato, E. B. (2016). An efficient K-NN approach for automatic drowsiness detection using single-channel EEG recording. *2016 38th Annual International Conference of the IEEE Engineering in Medicine and Biology Society (EMBC)*, 820-824. https://doi.org/10.1109/EMBC.2016.7590827

**Contact information:**

**Renyu YANG**, Senior Engineer, PhD
Guangdong University of Finance & Economics,
Guangzhou 510320, China
E-mail: 25198850@qq.com

**Ling ZHANG**, Senior Engineer, MS
Guangzhou Vocational College of Technology & Business,
Guangzhou 511442, China
E-mail: 258145593@ qq.com

**Boming ZHONG**, Graduate Student
Guangdong University of Finance & Economics,
Guangzhou 510320, China
E-mail: 1613462703@qq.com

**Lixing HOU**, Graduate Student
Guangdong University of Finance & Economics,
Guangzhou 510320, China
E-mail: 382518926@qq.com

**Donglong ZHU**, Graduate Student
Guangdong University of Finance & Economics,
Guangzhou 510320, China
E-mail: 2992357391@qq.com

**Jianliang MIN,** PhD
(Corresponding author)
Organ Transplantation Center, The First Affiliated Hospital,
Sun Yat-sen University, Guangzhou 510080, China
School of Medicine, Jiaying University, Meizhou 514015, China
E-mail: minjliang@mail2.sysu.edu.cn